22. Takemura, A., Inoue, Y., Kawano, K., Quaia, C. & Miles, F. A. Single-unit activity in cortical area MST associated with disparity-vergence eye movements: evidence for population coding. *J. Neurophysiol.* **85,** 2245–2266 (2001).
23. Colby, C. L., Duhamel, J. R. & Goldberg, M. E. Ventral intraparietal area of the macaque: anatomic location and visual response properties. *J. Neurophysiol.* **69,** 902–914 (1993).
24. Ferraina, S., Pare, M. & Wurtz, R. H. Disparity sensitivity of frontal eye field neurons. *J. Neurophysiol.* **83,** 625–629 (2000).
25. Kakei, S., Hoffman, D. S. & Strick, P. L. Direction of action is represented in the ventral premotor cortex. *Nature Neurosci.* **4,** 1020–1025 (2001).
26. Mushiake, H., Tanatsugu, Y. & Tanji, J. Neuronal activity in the ventral part of premotor cortex during target-reach movement is modulated by direction of gaze. *J. Neurophysiol.* **78,** 567–571 (1997).
27. Fogassi, L. *et al.* Space coding by premotor cortex. *Exp. Brain Res.* **89,** 686–690 (1992).
28. Fogassi, L. *et al.* Coding of peripersonal space in inferior premotor cortex (area F4). *J. Neurophysiol.* **76,** 141–157 (1996).
29. Graziano, M. S., Hu, X. T. & Gross, C. G. Visuospatial properties of ventral premotor cortex. *J. Neurophysiol.* **77,** 2268–2292 (1997).
30. Krauzlis, R. J. & Lisberger, S. G. Directional organization of eye movement and visual signals in the floccular lobe of the monkey cerebellum. *Exp. Brain Res.* **109,** 289–302 (1996).

Acknowledgements

We thank B. Cumming, M. Goldberg, S. Lisberger, F. Miles and P. Strick for comments on the manuscript, and T. Akao and F. Sato for participation in some experiments. This work was supported in part by CREST of JST, Japanese Ministry of Education, Science, Culture and Sports, and Marna Cosmetics.

Competing interests statement

The authors declare that they have no competing financial interests.

Correspondence and requests for materials should be addressed to K.F. (e-mail: kikuro@med.hokudai.ac.jp).

Loss of the Lkb1 tumour suppressor provokes intestinal polyposis but resistance to transformation

Nabeel Bardeesy*, Manisha Sinha*, Aram F. Hezel*, Sabina Signoretti†, Nathaniel A. Hathaway*, Norman E. Sharpless*, Massimo Loda†, Daniel R. Carrasco† & Ronald A. DePinho*

** Department of Adult Oncology, Dana-Farber Cancer Institute and Departments of Medicine and Genetics, Harvard Medical School, Boston, Massachusetts 02115, USA*

† Department of Pathology, Brigham and Women's Hospital, Harvard Medical School, Boston, Massachusetts 02115 USA

Germline mutations in *LKB1* (also known as *STK11*) are associated with Peutz–Jeghers syndrome (PJS), a disorder with predisposition to gastrointestinal polyposis and cancer[1]. PJS polyps are unusual neoplasms characterized by marked epithelial and stromal overgrowth but have limited malignant potential[2]. Here we show that *Lkb1*$^{+/-}$ mice develop intestinal polyps identical to those seen in individuals affected with PJS. Consistent with this *in vivo* tumour suppressor function, Lkb1 deficiency prevents culture-induced senescence without loss of *Ink4a/Arf* or *p53*. Despite compromised mortality, *Lkb1*$^{-/-}$ mouse embryonic fibroblasts show resistance to transformation by activated Ha-*Ras* either alone or with immortalizing oncogenes. This phenotype is in agreement with the paucity of mutations in *Ras* seen in PJS polyps[3,4] and suggests that loss of Lkb1 function as an early neoplastic event renders cells resistant to subsequent oncogene-induced transformation. In addition, the Lkb1 transcriptome shows modulation of factors linked to angiogenesis, extracellular matrix remodelling, cell adhesion and inhibition of *Ras* transformation. Together, our data rationalize several features of PJS polyposis—notably its peculiar histopathological presentation and limited malignant potential—and place Lkb1 in a distinct class of tumour suppressors.

Compared with other hereditary tumour syndromes, PJS has several unusual features. Although germline mutations in *LKB1* are associated with a cancer-prone condition[1,5], the *LKB1* gene is very rarely mutated or epigenetically silenced in sporadic tumours[6–8]. Heterozygosity for PJS is characterized by gastrointestinal polyps, but these polyps (hamartomas) possess low malignant potential and comprise disorganized non-dysplastic gastrointestinal mucosa with prominent branching smooth muscle components[2]. In addition, although gastrointestinal carcinomas develop with increased frequency in individuals with PJS, it is not clear whether hamartomas are precursor lesions of these carcinomas[2].

To investigate these paradoxical features of PJS, we generated mice carrying a conditional *Lkb1* allele (Fig. 1a, b). Mice carrying either one copy of the null allele (*Lkb1*$^{-}$) or a functional, floxed allele deleted for the *neomycin* resistance (*neo*^{r}) gene (*Lkb1*^{lox}) were generated in crosses with *EIIa–Cre*[9] or *CAGG–Flpe*[10] transgenic strains, respectively. Molecular analyses showed the expected recombinant alleles and absence of Lkb1 protein in mouse embryonic fibroblasts (MEFs) after Cre-mediated excision (Fig. 1c–e and see below). *Lkb1*$^{+/-}$ and *Lkb1*$^{lox/+}$ offspring were born at expected mendelian frequencies and showed no gross abnormalities. Consistent with previous results[11], *Lkb1*$^{-/-}$ mice had a lethal condition that manifested at about embryonic day (E) 8.5–11, with defects in vasculogenesis and placental development (data not shown).

We studied the tumour predisposition of these mice and found that 40 of 59 *Lkb1*$^{+/-}$ and 0 of 65 wild-type mice presented with symptoms of gastrointestinal obstruction at an average age of 43 weeks (Fig. 2a). Autopsy of symptomatic *Lkb1*$^{+/-}$ mice showed that polyps (between 1 and >15) were present throughout the gastrointestinal tract (Fig. 2b, c, and Supplementary Information Fig. 1), presenting as mucosal hamartomas with histological features mirroring those encountered in individuals with PJS or juvenile polyposis[2]. Detailed histopathological analysis failed to discern dysplastic or adenomatous changes in 15 polyps examined, and none of the polyps showed mutations in Ki-*ras* (Methods). A single *Lkb1*$^{+/-}$ mouse presented with a benign serous cystadenoma of the pancreas and two *Lkb1*$^{+/-}$ mice showed asymptomatic, benign uterine epithelial tumours (data not shown), but otherwise an extensive histological survey of 20 *Lkb1*$^{+/-}$ mice failed to identify additional neoplasms in other organs or abnormal mucocutaneous pigmentation up to an age of 45 weeks.

Hamartomas in individuals with PJS show loss of the wild-type *LKB1* allele in the epithelial compartment[3,4,12]. Correspondingly, laser capture microdissection (LCM) and allele-specific polymerase

Table 1 **Analysis of Lkb1 in polyps**

Tumour no.	LCM*	IHC*
1	Loss	Negative
2	Loss	Negative
3	Retention	Positive
4	Retention	Negative
5	Loss	ND
6	Retention	Negative
7	Retention	Negative
8	Retention	Positive
9	Retention	Positive
10	Retention	Positive
12	Retention	ND
13	Retention	Negative
14	ND	Negative
15	ND	Positive
16	ND	Negative
17	ND	Positive
Total	3/12	8/14

*Retention/loss denotes status of wild-type *Lkb1* allele. IHC, immunohistochemistry using an antibody against Lkb1; LCM, laser capture microdissection; ND, not determined or not informative.

 © 2002 Nature Publishing Group

chain reaction (PCR) analysis showed clear loss of the wild-type allele in the epithelial component of 3 of 12 polyps arising in *Lkb1*$^{+/-}$ mice (Fig. 2d, polyps 1, 2 and 5); analysis of the stromal component of polyp 2 showed that wild-type *Lkb1* had been retained (Fig. 2d, lane S2). To extend this molecular analysis, we evaluated the cellular expression of Lkb1. Immunohistochemistry of normal intestinal epithelium using an antibody against Lkb1 identified a gradient of Lkb1 expression, which was highest in the crypt cells and lowest in the postmitotic differentiated compartment (Fig. 2e, region below broken line), and expression in the stromal cells of the submucosal layer (data not shown). Immunoreactivity against Lkb1 in sections of whole bowel or cultured MEFs was predominantly perinuclear and cytoplasmic (Fig. 2f, h, note absence of signal in the *Lkb1*$^{-/-}$ MEFs). In 8 of 14 polyps, immunoreactivity against Lkb1 was absent in the polyp epithelium but consistently retained in the neighbouring stroma and normal crypt epithelial cells (Fig. 2e, f, and Table 1); notably, four of eight polyps that retained wild-type *Lkb*1 alleles showed a loss of immunoreactivity that was consistent with epigenetic gene silencing. In the polyps that retained expression of Lkb1 (Fig. 2g), other means of inactivation such as point mutations or microdeletions might be operative, although tumour promotion by haploinsufficiency remains a formal possibility.

Given the robust expression of Lkb1 in MEF cultures (Fig. 1e), we used a somatic deletion approach in this model system to evaluate the biological role of Lkb1. Early passage (<passage 5) *Lkb1*$^{-/-}$ and wild-type MEFs, cultivated under a 3T9 or 3T3 protocol, showed similar growth kinetics (Fig. 3a and data not shown). *Lkb1*$^{-/-}$ MEFs possessed a small but consistent increase in G1 content (6.1 ± 1.9%) and reciprocal reduction in G2 (7.4 ± 1.8%; Supplementary Information Fig. 2a). At later passage (>9), *Lkb1*$^{+/-}$ and wild-type cultures underwent growth arrest, whereas all six independently derived *Lkb1*$^{-/-}$ cultures showed unabated growth after more than 40 population doublings (Fig. 3a). Reconstitution of wild-type Lkb1, but not a kinase-dead Lkb1 mutant, restored the ability of early passage *Lkb1*$^{-/-}$ cultures to undergo passage-induced growth arrest (Fig. 3b). Despite their immortal growth on serial passage, early and late passage *Lkb1*$^{-/-}$ cells did not form colonies efficiently when seeded at very low densities (data not shown). This phenotype of density-dependent immortalization suggested that signals emanating from neighbouring cells might contribute to the immortalizing effects of Lkb1 deficiency.

The phenomenon of passage-induced senescence in MEFs has been attributed to the activation of a cellular stress response elicited by *in vitro* growth conditions[13,14], a process that depends on intact function of the p19^{Arf}/p53 and retinoblastoma (Rb) pathways[15–18]. Serially passaged *Lkb1*$^{-/-}$ MEFs showed a prominent reduction in accumulation of p53, p19^{Arf} and p16^{Ink4a} as compared with wild-type control cultures cultivated in parallel (Fig. 3c, d), and a diminished expression of the p53-induced gene *p21*^{Cip1} (data not shown). Notably, even in late passage (>20) *Lkb1*$^{-/-}$ MEFs, the p19^{Arf}/p53 pathway remained intact, as judged by p53 stabilization and growth arrest after exposure to various DNA-damaging agents (Fig. 3e and Supplementary Information Fig. 2c, d) or to ectopic expression of activated Ras, p19^{Arf} or c-Myc (Fig. 3f, g, and data not shown). Similarly, an intact Rb pathway in *Lkb1*$^{-/-}$ cells was suggested by normal expression and phosphorylation of Rb (data not shown), normal S-phase re-entry kinetics on refeeding after serum starvation (Supplementary Information Fig. 2b), and intact G1 arrest after DNA damage or enforced expression of p19^{Arf} (Supplementary Information Fig. 2c–e). Together, these data suggest that loss of Lkb1 immortalizes MEFs by attenuating the culture-shock induction of the *Ink4a/Arf* locus without directly impairing the function of p53 or Rb. A relationship between *Lkb1* and *Ink4a/Arf* was further suggested by the inability of Lkb1 to induce growth arrest in *Lkb1*$^{-/-}$ *Ink4a/Arf*$^{-/-}$ cells (data not shown).

MEFs with an intact p19^{Arf}/p53 pathway are sensitive to Ras-induced premature senescence, whereas cells with compromised mortality pathways are readily transformed by activated Ha-*ras* (H-

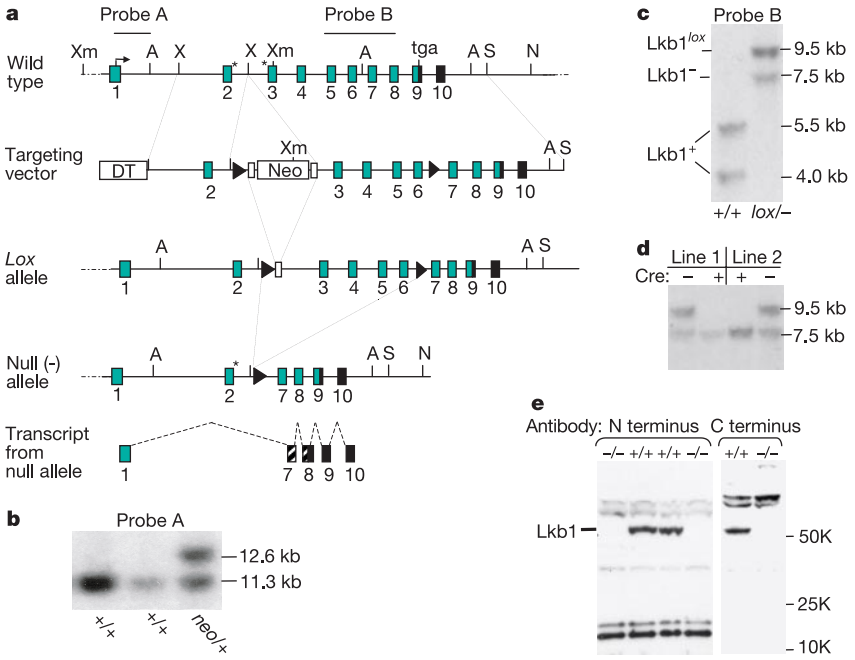

Figure 1 Targeting strategy and analysis of *Lkb1*. **a**, *Lkb1* genomic structure and recombinant alleles. The 3′ untranslated region (black bars), and noncanonical splice sequences (asterisks) are indicated. The transcript from the *Lkb1* null allele eliminates exons 2–6, resulting in a translational frameshift (crosshatched bars). **b**, Southern analysis of DNA from ES cell clones showing targeting of the *Lkb1* locus. **c**, Southern analysis of the *lox*, null (−), and wild-type (+) alleles. **d**, Southern analysis of DNA from *Lkb1*$^{lox/-}$ MEFs, untreated (−) or infected with a Cre retrovirus (+). **e**, Western analysis of *Lkb1*$^{lox/-}$ (−/−) and wild-type (+/+) MEFs after Cre expression, using antibodies to the amino (left) and carboxy (right) termini of Lkb1.

© 2002 Nature Publishing Group

RASV12)[15,19]. Unexpectedly, activated Ha-*ras* provoked premature senescence (that is, growth arrest and senescence-associated accumulation of β-galactosidase) in *Lkb1*$^{-/-}$ cells, even at late passage (>20), despite their immortal phenotype and attenuated expression of p53 and p19^{Arf} (Fig. 3f and data not shown). In addition, the transformation efficiency of activated Ha-*ras* in combination with the SV40 large T antigen (T-Ag), dominant-negative p53 (*p53-DD*) or adenovirus E1a was severely reduced in *Lkb1*$^{-/-}$ MEFs as compared with wild-type cultures (Fig. 4a, b). This resistance to transformation was also observed with T-Ag and a different dominantly acting oncogene, *Dbs*—a Dbl family guanine nucleotide exchange factor for Rho GTPases[20] (Fig. 4a, b). Furthermore, activated Ha-*ras* induced a marked decrease in growth of *Lkb1*$^{-/-}$ *Ink4a/Arf*$^{-/-}$ cells compared with wild-type *Ink4a/Arf*$^{-/-}$ cells (Fig. 4c). This decrease in proliferation was restored by reintroduction of Lkb1 with Ha-*ras* into *Lkb1*$^{-/-}$*ink4a/arf*$^{-/-}$ cells (Fig. 4c). These data indicate that Lkb1 deficiency unmasks a p19^{Arf}/p53-independent growth inhibitory pathway provoked by activated Ras.

The complex biological properties associated with Lkb1 deficiency prompted us to carry out transcriptional profiling of wild-type and *Lkb1*$^{-/-}$ MEFs, as well as polyps derived from *Lkb1*$^{+/-}$ mice (Supplementary Information Figs 3 and 4). *Lkb1*$^{-/-}$ MEFs and polyps showed prominent alterations in the expression of several broad classes of genes, most notably secreted signalling molecules and regulators of the extracellular matrix (ECM). In particular, many genes that show substantially altered expression in *Lkb1*$^{-/-}$ MEFs modulate the transformed phenotype of mesenchymal cells, which might explain the impaired transformation of *Lkb1*$^{-/-}$ cells by activated Ha-*ras*. For example, lumican, fibulin-1D and Igfbp5 are established potent inhibitors of fibroblast transformation[21–23]. *Lkb1*$^{-/-}$ cells also show diminished expression of the *p8* gene, which encodes an HMG-I/Y-like (high mobility group) protein that is required for *ras* transformation of MEFs[24]. Notably, increased expression of lumican and Igfbp5 in *Lkb1*$^{-/-}$ cells remained despite enforced expression of activated *ras* (Fig. 5b). These alterations in *ras*-modulated genes suggest a molecular basis for the resistance of *Lkb1*$^{-/-}$ MEFs to oncogene-induced transformation. Clearly, the absence of Lkb1 does not result in a fundamental disruption of activated *ras* signalling because the

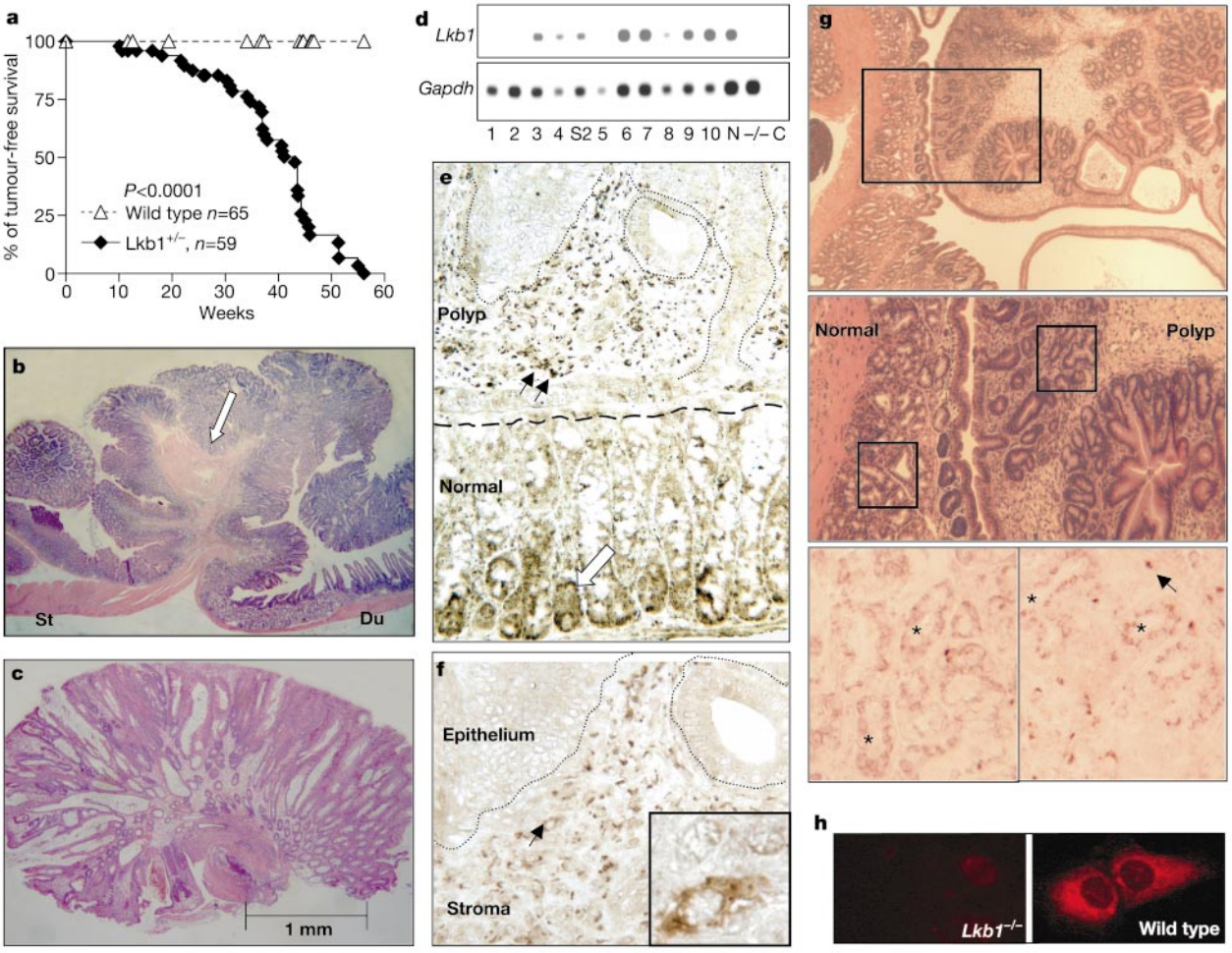

Figure 2 Gastrointestinal polyps in *Lkb1*$^{+/-}$ mice. **a**, Tumour-free survival (Kaplan–Meier) analysis. **b**, **c**, Sections of a pyloric polyp with smooth muscle splaying (**b**, arrow) and a colonic polyp showing mucosal disorganization with cystically dilated glands (**c**) stained with haematoxylin and eosin. Du, duodenum; St, stomach. **d**, Allele-specific PCR analysis of DNA isolated by LCM from polyp epithelium (1–10) or stroma (S2) for the presence of wild-type *Lkb1* and *Gapdh* control alleles. N, *Lkb1*$^{+/-}$ DNA; −/−, *Lkb1*$^{-/-}$ DNA; C, no DNA. At longer exposure to film, the *Lkb1* allele was detectable at hypomolar ratios in polyps 1 and 2. **e**, **f**, Immunoreactivity against Lkb1 is detected in normal colonic epithelium (thick arrow) and polyp stroma (thin arrows) but is undetectable in the epithelium of polyp 2 (dotted lines). **f**, Higher magnification view of **e**. Inset, cytoplasmic and perinuclear staining of a stromal cell. **g**, Top, small intestine (left) and adjacent polyp 9 (right) stained with haematoxylin and eosin. The boxed region is shown at higher magnification in the middle. Immunoreactivity against Lkb1 is detected (asterisks) both in the normal intestinal epithelium (bottom left) and the polyp epithelium (bottom right), as well as in the tumour stroma (arrow). **h**, Immunofluoresence of wild-type and *Lkb1*$^{-/-}$ MEFs shows the specificity of the perinuclear and cytoplasmic staining pattern.

© 2002 Nature Publishing Group

induction of a range of Ras targets such as Hb-Egf was comparable in wild-type and *Lkb1*$^{-/-}$ MEFs (Fig. 5b and data not shown).

Expression profiling of a series of polyps compared with adjacent intestine also showed numerous reproducible changes in gene expression (Supplementary Information Fig. 4). Notably, several genes, including Igfbp5, Pdgfr-α and *MMp2*, showed marked elevation in both *Lkb1*$^{-/-}$ MEFs and in polyps (Fig. 5c and not shown). Collectively, these datasets point to clear parallels between the MEFs and polyps to the extent that they highlight alterations in regulators of the cellular microenvironment and in pathways that influence *ras* transformation.

Given the preponderance of ECM regulators and secreted signalling molecules among the genes showing elevated expression in *Lkb1*$^{-/-}$ cells, we wanted to determine whether the conditioned media from these cells could exert paracrine effects on gene expression. This issue is particularly relevant given the retention of *Lkb1* in the highly reactive stromal compartment of PJS polyps. Northern blot analysis showed that expression of MMP2 is increased in *Lkb1*$^{-/-}$ MEFs regardless of the culture media source (Fig. 5d). Conversely, cultivation of wild-type cells in the conditioned media from *Lkb1*$^{-/-}$ cells produced a significant increase in MMP2 as compared with that detected after growth in conditioned media from wild-type MEFs; by contrast, Igfbp5 was unaffected in this experiment (Fig. 5d).

In support of this observation, a marked increase in MMP2 could be seen in the stroma of polyps from *Lkb1*$^{+/-}$ mice (data not shown). Consistent with a previous report[11], we also noted a fourfold increase in the amount of vascular endothelial growth factor (Vegf) in the conditioned media from *Lkb1*$^{-/-}$ MEFs (data not shown), but no difference in steady-state levels of *Vegf* mRNA (Fig. 5a), suggesting an increased release of Vegf resulting from higher MMP activity in *Lkb1*$^{-/-}$ cultures[25]. These observations are in keeping with the idea that, *in vivo*, Lkb1-deficient cells may elicit alterations in signalling and ECM composition in the proximal stromal microenvironment.

Here we have modelled PJS intestinal polyposis and evaluated the biological and oncogenic impact of Lkb1 deficiency. We show that *Lkb1*$^{+/-}$ mice develop intestinal polyps that are indistinguishable from those in individuals affected with PJS including a complete absence of dysplastic changes and activating *ras* mutations. Paradoxically, although Lkb1 deficiency confers immortal growth with retention of classical mortality pathways, *Lkb1*$^{-/-}$ MEFs retain sensitivity to Ras-induced senescence and show resistance to the transforming effects of activated *ras* alone or in combination with an array of powerful immortalizing oncoproteins including T-Ag. This observation has added significance because, in contrast to

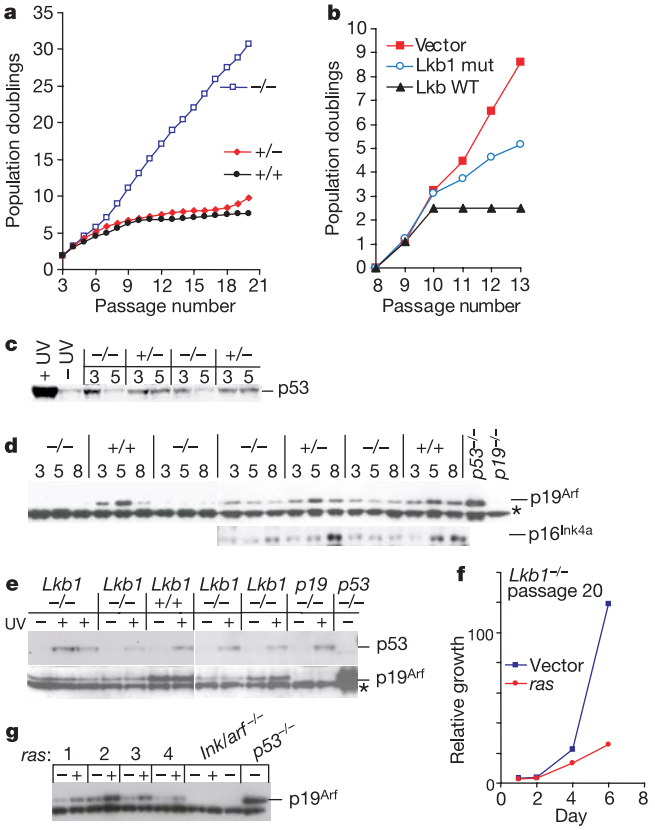

Figure 3 *Lkb1*$^{-/-}$ MEF immortalization studies. **a**, Representative results of MEF cultures of the different *Lkb1* genotypes passaged on a 3T9 protocol. **b**, Growth of *Lkb1*$^{-/-}$ MEFs after retroviral expression of wild type (WT) or the kinase-dead Lys78Ile Lkb1 mutant (mut). **c**, Western blot analysis of p53 in serially passaged MEF lines. The *Lkb1* genotypes are indicated. Control lysates were irradiated (+UV) or untreated (−UV) MEF cultures. **d**, Western blot analysis of p19^{Arf} and p16^{Ink4a} in several, serially passaged MEF lines. Asterisk denotes a nonspecific immunoreactive band. *p53*$^{-/-}$ and *p16*^{Ink4a}/*p19*$^{Arf-/-}$ (labelled p19$^{Arf-/-}$) MEFs are controls for immunoreactivity against p19^{Arf}. **e**, Intact *p19*^{Arf} and *p53* loci in late passage *Lkb*$^{-/-}$ MEFs. Top, induction of p53 by ultraviolet light (UV) in passage 20 *Lkb1*$^{-/-}$ MEFs. The wild-type (+/+) lysate is from passage 14. Bottom, expression of p19^{Arf}. **f**, Activated Ha-*ras* causes growth arrest in passage 20 *Lkb1*$^{-/-}$ MEFs. Data are representative of four MEF lines. **g**, Western blot showing induction of p19^{Arf} in passage 20 *Lkb1*$^{-/-}$ MEFs lines infected with retroviruses encoding activated Ha-*ras* or empty vector (−).

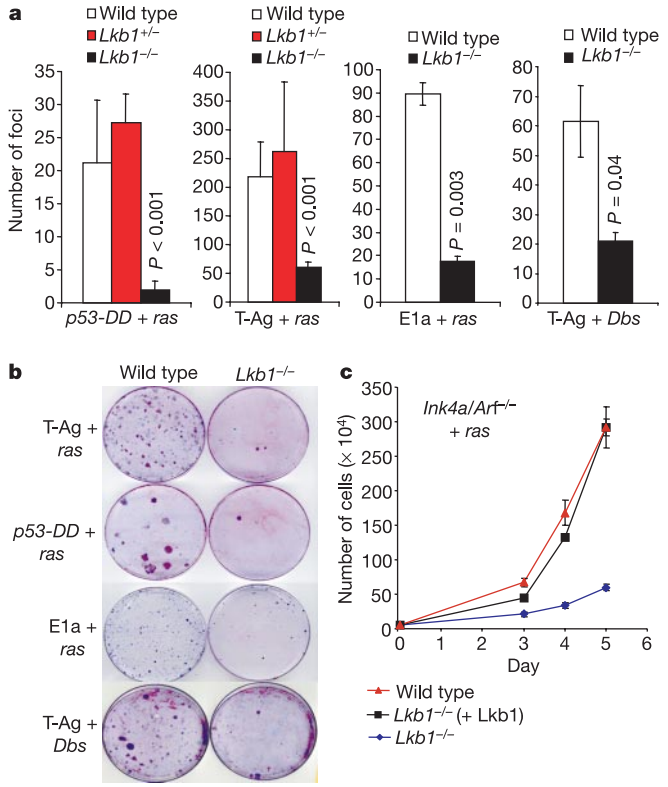

Figure 4 *Lkb1*$^{-/-}$ cells are resistant to oncogenic transformation. **a**, Transformation assays. Values represent the mean number of transformed foci obtained for each *Lkb1* genotype in transformation assays with the indicated oncogenes. **b**, Representative plates stained with Giemsa from transformation assays. **c**, Growth curve of MEFs seeded at 50,000 per 10-cm dish after infection with Ha-*ras*. The genetic background of all cells was *Ink4a/Arf*$^{-/-}$ and wild-type, *Lkb1*$^{-/-}$ or *Lkb1*$^{-/-}$ with reconstituted wild-type *Lkb1*.

© 2002 Nature Publishing Group

other gastrointestinal neoplasms in humans, polyps arising in people affected with PJS rarely, if ever, carry oncogenic *ras* mutations[3,4].

In summary, Lkb1 has a complex role in growth and transformation. Outwardly, the resistance to activated *ras* transformation and impaired malignant progression may seem difficult to reconcile with the polyposis and carcinoma-prone condition provoked by Lkb1 deficiency. On further consideration, this paradoxical picture is consistent with the notable clinical features of PJS and its distinctive cancer genetics. Although individuals with PJS have a significantly increased risk of developing carcinomas, the PJS polyps themselves rarely show features of dysplasia[2]. Our data indicate that there may be limitations on the type of initiating and/or cooperating events that are required for the malignant transformation of *LKB1* $^{-/-}$ cells, despite the immortalizing effects of loss of *LKB1*. The extremely rare inactivation of *LKB1* in tumours other than those of individuals carrying germline mutations may also point to a constrained genetic context wherein *LKB1* loss enables malignant transformation[6–8]. Given the increased incidence of carcinoma associated with germline *LKB1* mutations, an additional implication of our studies is that the order of mutational events may be an important parameter in dictating the type of cooperating mutations and the malignant potential of the initiated neoplasm: early loss of *LKB1* may promote strictly benign neoplasia, whereas loss of *LKB1* in a later stage lesion could facilitate malignant progression. We therefore propose that *LKB1* is a context-dependent tumour suppressor gene, whose loss of function facilitates evasion of a classical barrier to neoplasia (senescence) and engenders a tumour-like stromal environment, but renders cells resistant to transformation by powerful oncogenic combinations.

Note added in proof: After this manuscript was submitted, Myoshi *et al.*[29] and Jishage *et al.*[30] reported gastrointestinal polyps in *Lkb1* heterozygous mice; in contrast to our detection of Lkb1 loss in a subset of polyps, these studies reported retention of Lkb1 in the polyps analysed (2 and 3 polyps, respectively). □

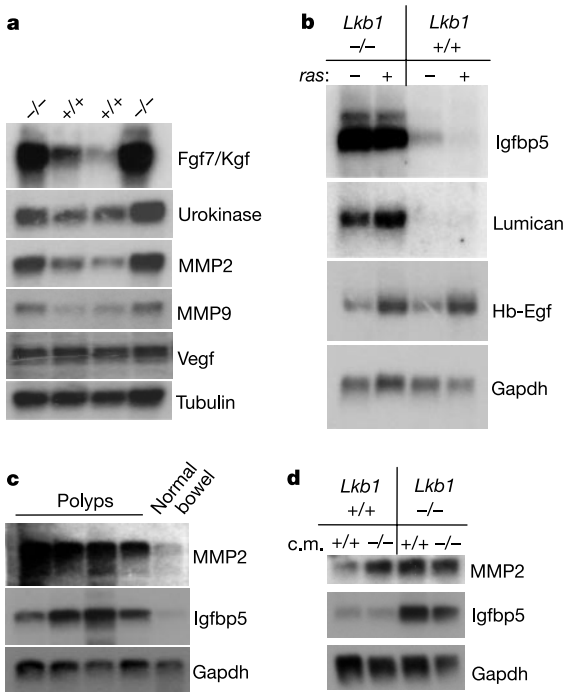

Figure 5 *Lkb1* $^{-/-}$ expression profile. **a**, Northern blot analyses of candidate regulators of angiogenesis and extracellular matrix remodelling in wild-type and *Lkb1* $^{-/-}$ MEFs. **b**, Expression of modulators of Ha-*ras* transformation in wild-type and *Lkb1* $^{-/-}$ MEFs. Cells were either transduced with retroviruses expressing Ha-*ras* (H-RASV12, +) or with empty vector (−). **c**, Northern blot analysis of gastrointestinal polyps and normal bowel from *Lkb1* $^{+/-}$ mice. **d**, Conditioned media from *Lkb1* $^{-/-}$ cells induces MMP2 expression in *Lkb1* $^{+/+}$ MEFs. Wild-type and *Lkb1* $^{-/-}$ MEFs were cultured in conditioned media (c.m.) from either genotype and analysed by northern blot.

Methods

Targeting construct, colony generation and genotyping

We cloned and mapped the *Lkb1* locus from a bacterial artificial chromosome library. The targeting vector (Fig. 1a) carried a negative selection marker for diptheria toxin (DT), a positive selection marker for neomycin acetyltransferase (Neo), Frt sites (white rectangles) and *loxP* sites (black triangles). The restriction sites were *Xmn*I (Xm), *Xba*I (X), *Avr*II (A), *Sma*I (S), *Not*I (N). We electroporated TC1 embryonic stem (ES) cells and selected transformed cells by standard techniques. We screened 92 clones by Southern analysis using a *Xmn*I restriction enzyme and a 5′ fragment external to the targeting construct (Fig. 1a, b, probe A) to identify nine recombinants. Blastocyst injections were carried out with three different targeted clones, and transmitting chimaeric mice were bred from *CAGG–Flpe* and *EIIa–Cre* transgenic mice[9,10] to generate the *Lkb1* ^{lox} and *Lkb1* $^{-}$ alleles, respectively (Fig. 1a). *Cre* $^{+}$ *Lkb1* $^{+/-}$ and *Flpe* $^{+}$ *Lkb1* $^{lox/+}$ males were backcrossed one or two times to FVB/n females and progeny of these matings that were *Cre* $^{-}$ or *Flpe* $^{-}$ were then backcrossed to littermates to yield the experimental cohort. Mice were genotyped by Southern analysis and multiplex PCR (primers and conditions are available from R.A.D. on request). Colonies were observed three times per week for morbidity, and autopsied for overt tumour or illness. Stool specimens were monitored weekly for occult blood using Hemoccult slides (Beckman Coulter).

Cellular analysis

We generated MEFs from 13.5 post-coitum embryos and grew them in DMEM medium plus 10% fetal calf serum (Hyclone), 50 μM β-mercaptoethanol, penicillin and streptomycin. As *Lkb1* $^{-/-}$ embryos did not develop past 11.5 days post coitum, *Lkb1* $^{-/-}$ MEFs were produced by *in vitro* excision of the *Lkb1* ^{lox} allele using a self-excising Cre expressing retrovirus[26]. *Lkb1* $^{lox/-}$ and littermate control *Lkb1* $^{lox/+}$ and wild-type cultures were exposed to Cre retrovirus at passage 2 and found to sustain 95–100% deletion of the *Lkb1* ^{lox} allele in short-term and 100% deletion in long-term passage cultures as determined by western blot, Southern blot and PCR analysis (Fig. 1d and data not shown). The structure of the transcript arising from the *Lkb1* null allele (Fig. 1a) was determined by PCR with reverse transcription and sequence analysis. For 3T9 or 3T3 analysis, 3×10^5 cells were passaged into six-well or 6-cm dishes, every 3 d. At least five independent lines were assayed per genotype, with three independent cultures per line. Senescence was determined as described[27]. Growth curves were generated by seeding 25,000 cells per well in 12-well plates, each line in triplicate. We fixed plates on the indicated day, stained them with crystal violet, extracted them with 10% acetic acid, and measured the relative cell number at an absorbance of 595 nm. For S-phase re-entry experiments, passage 5 MEFs at 80% confluency were serum starved for 72 h and then stimulated by subculturing into serum-containing medium. Retroviral transduction, low-density seeding, SA-β-galactosidase, Ras-induced growth arrest and transformation assays were done as described[27]. Transient transfection efficiencies did not differ between wild-type and *Lkb1* $^{-/-}$ cells, as determined using green fluorescent protein. We used retroviruses for the E1a–*ras* transformation assay and for expression of Lkb1.

Molecular analysis

Cell lysates from MEFs were prepared and resolved on polyacrylamide gels as described[27]. Western blots of Lkb1 were carried out using antibodies D19 (Santa Cruz) or 07-093 (Upstate), or using 1G, a rabbit polyclonal antibody raised against the carboxy terminus of Lkb1; other proteins were blotted as described[27]. Loading was assessed using α-tubulin (Sigma). For p53 induction, lysates were collected 12 h after exposure to ultraviolet radiation (100 μJ M $^{-2}$). Immunohistochemistry was carried out on paraffin-embedded sections as described[28] except that antigen retrieval was carried out in Tris-EDTA, pH 6.8, at 90 °C for 30 min using antibody D19. We measured the immunofluorescence of Lkb1 as described[28], using antibody D19 or 1G.

Expression profiling was carried out using the Affymetrix U74-A chip, and data were analysed using Affymetrix GeneChip 3.1 software. We isolated RNA from two pairs of littermate *Lkb1* $^{-/-}$ and wild-type MEF cultures at passage 5. Expression changes were considered significant only if the GeneChip software made the call of 'different' and if the expression differences were greater than twofold in both sets of MEFs. Profiling of polyps versus adjacent normal intestine was done on four paired sets of specimens. Expression analysis was also carried out using nylon cDNA arrays according to the manufacturer's instructions (arrays MM001, MM006, MM009 and MM010; Superarray).

For LCM, paraffin-embedded 5-μm sections were removed from paraffin by xylene, washed with ethanol, rehydrated in deionized water and stained with haematoxylin and eosin. Epithelial and stromal cells from the polyps and normal epithelial cells from the adjacent mucosa were microdissected using the PixCell II Laser Capture Microdissection System (Acturus Engineering). About 500–1,000 cells were digested in 30 μl of buffer containing 10 mM Tris, 1 mM EDTA, 1% Tween 20 with 1 mg ml $^{-1}$ proteinase K at 37 °C for 12 h. Samples were heated to 94 °C for 10 min and then centrifuged. We used 3 μl of the supernatant used as template for PCR (20 cycles) with primers specific for the *Lkb1* wild-type allele or to *Gapdh* and subjected the products to Southern blotting. LCM was repeated for all specimens to verify the results. For Ki-*ras* mutational analysis, exons 1 and 2 of Ki-*ras* were amplified by PCR from LCM material and sequenced.

© 2002 Nature Publishing Group

Received 5 April; accepted 10 July 2002; doi:10.1038/nature01045.

1. Hemminki, A. *et al.* A serine/threonine kinase gene defective in Peutz–Jeghers syndrome. *Nature* **391,** 184–187 (1998).
2. Cooper, H. S. *Pathology of the Gastrointestinal Tract* (eds Ming, S.-C. & Goldman, H.) 819–853 (Wiliams & Wilkens, Baltimore, 1998).
3. Entius, M. M. *et al.* Molecular genetic alterations in hamartomatous polyps and carcinomas of patients with Peutz–Jeghers syndrome. *J. Clin. Pathol.* **54,** 126–131 (2001).
4. Gruber, S. B. *et al.* Pathogenesis of adenocarcinoma in Peutz–Jeghers syndrome. *Cancer Res.* **58,** 5267–5270 (1998).
5. Giardiello, F. M. *et al.* Very high risk of cancer in familial Peutz–Jeghers syndrome. *Gastroenterology* **119,** 1447–1453 (2000).
6. Avizienyte, E. *et al.* Somatic mutations in LKB1 are rare in sporadic colorectal and testicular tumors. *Cancer Res.* **58,** 2087–2090 (1998).
7. Avizienyte, E. *et al.* LKB1 somatic mutations in sporadic tumors. *Am. J. Pathol.* **154,** 677–681 (1999).
8. Esteller, M. *et al.* Epigenetic inactivation of LKB1 in primary tumors associated with the Peutz–Jeghers syndrome. *Oncogene* **19,** 164–168 (2000).
9. Lakso, M. *et al.* Efficient *in vivo* manipulation of mouse genomic sequences at the zygote stage. *Proc. Natl Acad. Sci. USA* **93,** 5860–5865 (1996).
10. Rodriguez, C. I. *et al.* High-efficiency deleter mice show that FLPe is an alternative to *Cre–loxP. Nature Genet.* **25,** 139–140 (2000).
11. Ylikorkala, A. *et al.* Vascular abnormalities and deregulation of VEGF in Lkb1-deficient mice. *Science* **293,** 1323–1326 (2001).
12. Hemminki, A. *et al.* Localization of a susceptibility locus for Peutz–Jeghers syndrome to 19p using comparative genomic hybridization and targeted linkage analysis. *Nature Genet.* **15,** 87–90 (1997).
13. Ramirez, R. D. *et al.* Putative telomere-independent mechanisms of replicative aging reflect inadequate growth conditions. *Genes Dev.* **15,** 398–403 (2001).
14. Sherr, C. J. & DePinho, R. A. Cellular senescence: mitotic clock or culture shock? *Cell* **102,** 407–410 (2000).
15. Kamijo, T. *et al.* Tumor suppression at the mouse INK4a locus mediated by the alternative reading frame product $p19^{ARF}$. *Cell* **91,** 649–659 (1997).
16. Serrano, M. *et al.* Role of the INK4a locus in tumour suppression and cell mortality. *Cell* **85,** 27–37 (1996).
17. Sage, J. *et al.* Targeted disruption of the three *Rb*-related genes leads to loss of G_1 control and immortalization. *Genes Dev.* **14,** 3037–3050 (2000).
18. Dannenberg, J. H., van Rossum, A., Schuijff, L. & te Riele, H. Ablation of the retinoblastoma gene family deregulates G_1 control causing immortalization and increased cell turnover under growth-restricting conditions. *Genes Dev.* **14,** 3051–3064 (2000).
19. Serrano, M., Lin, A. W., McCurrach, M. E., Beach, D. & Lowe, S. W. Oncogenic *ras* provokes premature cell senescence associated with accumulation of p53 and $p16^{INK4a}$. *Cell* **88,** 593–602 (1997).
20. Whitehead, I. P. *et al.* Dependence of Dbl and Dbs transformation on MEK and NF-κB activation. *Mol. Cell. Biol.* **19,** 7759–7770 (1999).
21. Yoshioka, N. *et al.* Isolation of transformation suppressor genes by cDNA subtraction: lumican suppresses transformation induced by v-*src* and v-K-*ras. J. Virol.* **74,** 1008–1013 (2000).
22. Qing, J. *et al.* Suppression of anchorage-independent growth and matrigel invasion and delayed tumour formation by elevated expression of fibulin-1D in human fibrosarcoma-derived cell lines. *Oncogene* **15,** 2159–2168 (1997).
23. Reeve, J. G., Guadano, A., Xiong, J., Morgan, J. & Bleehen, N. M. Diminished expression of insulin-like growth factor (IGF) binding protein-5 and activation of IGF-I-mediated autocrine growth in simian virus 40-transformed human fibroblasts. *J. Biol. Chem.* **270,** 135–142 (1995).
24. Vasseur, S. *et al.* p8 is critical for tumour development induced by rasV12 mutated protein and E1A oncogene. *EMBO Rep.* **3,** 165–170 (2002).
25. Bergers, G. *et al.* Matrix metalloproteinase-9 triggers the angiogenic switch during carcinogenesis. *Nature Cell Biol.* **2,** 737–744 (2000).
26. Silver, D. P. & Livingston, D. M. Self-excising retroviral vectors encoding the Cre recombinase overcome Cre-mediated cellular toxicity. *Mol. Cell* **8,** 233–243 (2001).
27. Sharpless, N. E. *et al.* Loss of $p16^{Ink4a}$ with retention of $p19^{Arf}$ predisposes mice to tumorigenesis. *Nature* **413,** 86–91 (2001).
28. Carrasco, D., Weih, F. & Bravo, R. Developmental expression of the mouse c-*rel* proto-oncogene in hematopoietic organs. *Development* **120,** 2991–3004 (1994).
29. Miyoshi, H. *et al.* Gastrointestinal hamartomatous polyposis in Lkb1 heterozygous knockout mice. *Cancer Res.* **62,** 2261–2266 (2002).
30. Jishage, K. *et al.* Role of Lkb1, the causative gene of Peutz-Jegher's syndrome, in embryogenesis and polyposis. *Proc. Natl Acad. Sci. USA* **99,** 8903–8908 (2002).

Supplementary Information accompanies the paper on *Nature*'s website (http://www.nature.com/nature).

Acknowledgements

We thank L. Ritchie and J. Horner of DFCI mouse core for advice and assistance; S. Dymecki, H. Westphal, M. Oren, S. Lowe, D. Silver, C. Der & J. DeCaprio for advice and reagents; and D. Livingston, J. DeCaprio and W. Kaelin for comments on the manuscript. N.B. is supported by the ACS John Peter Hoffman Award and the Liss Family Fund grant for research in pancreatic cancer. R.A.D. is an American Cancer Society Professor and recipient of the Steven and Michele Kirsch Foundation Investigator Award. This work was supported by grants from the NCI (National Cancer Institute) and ACS (American Cancer Society).

Competing interests statement

The authors declare that they have no competing financial interests.

Correspondence and requests for materials should be addressed to R.A.D. (e-mail: ron_depinho@dfci.harvard.edu).

SINAT5 promotes ubiquitin-related degradation of NAC1 to attenuate auxin signals

Qi Xie*, Hui-Shan Guo*, Geza Dallman*, Shengyun Fang†, Allan M. Weissman† & Nam-Hai Chua‡

* *Laboratory of Molecular Cell Biology, Temasek Life Sciences Laboratory, National University of Singapore, 1 Research Link, 117604 Singapore*
† *Regulation of Protein Function Laboratory, Center for Cancer Research, National Cancer Institute, Bethesda, Maryland 20892, USA*
‡ *Laboratory of Plant Molecular Biology, Rockefeller University, 1230 York Avenue, New York, New York 10021, USA*

The plant hormone indole-3 acetic acid (IAA or auxin) controls many aspects of plant development, including the production of lateral roots[1–3]. Ubiquitin-mediated proteolysis has a central role in this process. The genes *AXR1* and *TIR1* aid the assembly of an active SCF (Skp1/Cullin/F-box) complex that probably promotes degradation of the AUX/IAA transcriptional repressors in response to auxin[4–8]. The transcription activator NAC1, a member of the NAM/CUC family of transcription factors, functions downstream of TIR1 to transduce the auxin signal for lateral root development[9]. Here we show that SINAT5, an *Arabidopsis* homologue of the RING-finger *Drosophila* protein SINA, has ubiquitin protein ligase activity and can ubiquitinate NAC1. This activity is abolished by mutations in the RING motif of SINAT5. Overexpressing SINAT5 produces fewer lateral roots, whereas overexpression of a dominant-negative Cys49 → Ser mutant of SINAT5 develops more lateral roots. These lateral root phenotypes correlate with the expression of NAC1 observed *in vivo*. Low expression of NAC1 in roots can be increased by treatment with a proteasome inhibitor, which indicates that SINAT5 targets NAC1 for ubiquitin-mediated proteolysis to downregulate auxin signals in plant cells.

To investigate NAC1 action, we carried out yeast two-hybrid assays using NAC1 as a bait. One protein that interacted with NAC1 showed extensive sequence homology to two C3HC4 RING-finger proteins, SINA from *Drosophila*[10] and SIAH from human[11]. Because the gene encoding this protein is located on chromosome 5 we designated this protein SINA of *Arabidopsis thaliana* 5 (SINAT5, AF480944; Fig. 1a). The identities between SINAT5 and SINA (M38384) and SIAH (U76247) are 33% and 36%, respectively.

When SINAT5 was used as the bait, it interacted with the *Arabidopsis* AtUBC9A (AF480945; a protein that shows homology to members of the yeast Ubc4/5 and human UbcH5 families), ubiquitin (data not shown) and with itself (Fig. 1b). The carboxy-terminal region was responsible for SINAT5 dimerization (data not shown), which is consistent with results reported for SIAH[12,13]. We verified the dimerization of SINAT5 and interaction of the dimer with NAC1 by *in vitro* pull-down assays (Fig. 1c, d).

We determined the expression profile of *SINAT5* by generating transgenic plants carrying a fusion of the *SINAT5* promoter and the β-glucuronidase gene (*GUS*). *SINAT5–GUS* was expressed in low amounts in the vascular tissues of mature roots (Fig. 1e). But on treatment with auxin, expression was also detected in lateral root initials and in the elongation zone of the main root (Fig. 1e). This root expression pattern is very similar to that of *NAC1* after induction by auxin (ref. 9 and Fig. 1e), which suggests that SINAT5 and NAC1 function in the same types of cell. As for *NAC1*, expression of *SINAT5* was induced by auxin but more slowly (Fig. 1f).

To investigate the subcellular localization of SINAT5, we constructed a fusion of the green fluorescent protein (GFP) gene and

© 2002 Nature Publishing Group